Thermochimica Acta, 100 (1986) 119–148
Elsevier Science Publishers B.V., Amsterdam – Printed in The Netherlands

THERMAL DECOMPOSITION OF THE SOLVENT-EXTRACTED METAL COMPLEXES WITH HIGH MOLECULAR WEIGHT AMINES

TAICHI SATO

Department of Applied Chemistry, Faculty of Engineering, Shizuoka University, Hamamatsu (Japan)

(Received 3 January 1986)

ABSTRACT

Organic solutions from the extractions of divalent manganese, cobalt, copper and zinc, trivalent gallium, indium and thallium, tetravalent vanadium and zirconium, and hexavalent uranium and molybdenum with trioctylamine (TOA, R_3N) and trioctylmethylammonium chloride (TOMAC, $R_3R'NCl$) in benzene were heated in vacua to prepare benzene-free complexes. The resulting complexes were examined by thermogravimetry and differential thermal analysis under an atmosphere of nitrogen, and their thermally decomposed products, such as volatile matters and residues, by gas chromatography, X-ray diffraction and infrared spectroscopy. Consequently, the thermal decomposition process of these complexes is discussed and the structure of the complexes is proposed on the basis of the results obtained.

INTRODUCTION

Although the liquid–liquid extraction of metal with long-chain aliphatic amines has been investigated by many workers, the properties of the complexes isolated from their organic solutions have rarely been examined. In particular, studies on their thermal decomposition to obtain further information on their composition have been limited to the sulphato and nitrato complexes of uranium(VI) [1] and the chloro complexes of divalent manganese, cobalt, copper and zinc [2,3], vanadium(IV) [4,5], zirconium(IV) [6] and uranium(VI) [7,8]. Therefore the present paper extends the work to the chloro complexes of divalent manganese, cobalt, copper and zinc, trivalent gallium, indium and thallium, tetravalent vanadium and zirconium, and hexavalent uranium and molybdenum with trioctylamine (TOA, R_3N) and trioctylmethylammonium chloride (TOMAC, $R_3R'NCl$).

EXPERIMENTAL

Reagents

TOA and TOMAC (both > 99%, Koei Chemical Co., Ltd., Osaka) of high purity were used without further purification and diluted with benzene.

0040-6031/86/$03.50

Aqueous solutions of metals were prepared by dissolving their chlorides ($MnCl_2 \cdot 4H_2O$, $CoCl_2 \cdot 6H_2O$, $CuCl_2 \cdot 2H_2O$, $InCl_3$, $TlCl_3$, $VOCl_2$, $ZrCl_4$, UO_2Cl_2 except sodium molybdate ($Na_2MoO_4 \cdot 2H_2O$), molybdic acid ($H_2MoO_4 \cdot H_2O$) and gallium metal (99.9999%, Swiss Aluminium Ltd., Switzerland)) in hydrochloric acid solutions. All chemicals used were of analytical grade.

Preparation of the complexes

On the basis of the distribution data [9–18], the organic solutions saturated with divalent, trivalent, tetravalent and hexavalent metals with TOA and TOMAC were prepared by equilibrium at 20°C as follows. For manganese, cobalt, copper and zinc, 0.1 mol l^{-1} TOA or TOMAC in benzene was shaken for 10 min with the aqueous solutions containing 200 g l^{-1} $MnCl_2$ in 8 mol l^{-1} HCl, 200 g l^{-1} $CoCl_2$ in 8 mol l^{-1} HCl, 200 g l^{-1} $CuCl_2$ in 6 mol l^{-1} HCl or 100 g l^{-1} $ZnCl_2$ in 3 mol l^{-1} HCl and the organic phase separated centrifugally was shaken again with the fresh aqueous solutions so that they might be saturated with divalent metals. For gallium, indium and thallium, 0.05 mol l^{-1} TOA or TOMAC in benzene was shaken for 15 min with the aqueous solutions containing 0.085 mol l^{-1} $GaCl_3$ in 5 mol l^{-1} HCl, 0.226 mol l^{-1} $InCl_3$ in 6 mol l^{-1} HCl (or 5 mol l^{-1} HCl for TOMAC) or 0.048 mol l^{-1} in 0.1 mol l^{-1} HCl (or 0.01 mol l^{-1} HCl for TOMAC), and the organic phase was centrifuged. For vanadium, 0.05 mol l^{-1} TOA or TOMAC in benzene was shaken for 10 min with an aqueous solution of 0.1 mol l^{-1} $VOCl_2$ in 0.06 mol l^{-1} HCl containing 9.8 mol l^{-1} LiCl, and the organic phase was centrifuged and shaken again with a fresh aqueous solution, and then the procedure was repeated twelve times. For zirconium, 0.05 mol l^{-1} TOA or 0.082 mol l^{-1} TOMAC in benzene was shaken for 10 min with the aqueous solutions containing 0.02 mol l^{-1} $ZrCl_4$ in 10 and 8 mol l^{-1}, respectively, and the organic phase separated from the aqueous phase by centrifuging was equilibrated again with the fresh aqueous solutions, and then the procedure was repeated ten times. For uranium, 0.05 mol l^{-1} TOA or TOMAC in benzene was shaken for 10 min with the aqueous solutions of 0.1 mol l^{-1} UO_2Cl_2 in 3 and 7 mol l^{-1} HCl, respectively, and the organic phase was separated from aqueous phases by centrifuging. For molybdenum, however, since the results for the extractions of molybdenum(VI) from hydrochloric acid solutions by TOA and TOMAC suggested that the composition of the complex formed in the extraction at low aqueous acidity is different from that at higher acidity [18], the respective complexes with TOA and TOMAC were prepared from the following organic solutions obtained in the extractions at low and higher aqueous acidities: at low aqueous acidity, 0.01 mol l^{-1} TOA or TOMAC is benzene was shaken for 10 min with an aqueous solution containing 0.0062 mol l^{-1} Na_2MoO_4 in 0.015 mol l^{-1} (at pH 2.36), and the organic phase was shaken

TABLE 1

Variation of the molar ratios of $[R_3N]$ or $[R_3R'N]/[Cl]/[M]$ [a] in divalent metal saturated organic solutions from solvent extraction with TOA and TOMAC

Metal	Molar ratio	
	$[R_3N]/[Cl]/[M]$	$[R_3R'N]/[Cl]/[M]$
Mn(II)	2.1/4.0/1.0	2.0/4.0/1.0
Co(II)	2.0/4.3/1.0	2.0/3.6/1.0
Cu(II)	1.9/3.9/1.0	2.1/4.0/1.0
Zn(II)	2.0/3.8/1.0	1.8/3.4/1.0

[a] M = Mn, Co, Cu and Zn.

again with the fresh aqueous solution, and then the procedures were repeated seven times; at higher aqueous acidity, 0.05 mol l^{-1} TOA and TOMAC in benzene was shaken for 10 min with an aqueous solution of 0.2 mol l^{-1} H_2MoO_4 in 6 mol l^{-1} HCl, and the organic phase was separated from aqueous phase by centrifuging.

The organic phases so obtained were heated in vacua at 50–60°C to remove benzene. The resulting complexes, freed from benzene, contain the composition of extractant/chloride/metal in the molar ratios, indicating the stoichiometries to be $(R_3NH)_2MCl_4$ and $(R_3R'N)_2MCl_4$ (M = Mn, Co, Cu and Zn), respectively, shown in Table 1 [2,3]; $R_3NHGaCl_4$, $(R_3NH)_2InCl_5$, $R_3NHTlCl_4$, $R_3R'NGaCl_4$, $R_3R'NInCl_4$ and $R_3R'NTlCl_4$; $[R_3NHVO(OH)Cl_2]_2$ and $[R_3R'NVO(OH)Cl_2]_2$ [4,5]; $(R_3NH)_2ZrCl_6$ and $(R_3R'N)_2ZrCl_6$ [6]; $(R_3NH)UO_2Cl_4$ and $(R_3R'N)_2UO_2Cl_4$ [7,8]; $(R_3NH)Mo_nO_{3n}(OH)_2(H_2O)_n \cdot xH_2O$ and $(R_3R'N)Mo_nO_{3n}(OH)_2(H_2O)_n \cdot xH_2O$ and/or $(R_3NH)Mo_nO_{2(n+1)}(OH)_{2(n-1)} \cdot yH_2O$ and $(R_3R'N)Mo_nO_{2(n+1)}(OH)_{2(n-1)} \cdot yH_2O$ ($n = 1$–3) at low aqueous acidity; $(R_3NH)MoO_2Cl_3$ and $(R_3R'N)MoO_2Cl_3 \cdot xH_2O$ at higher aqueous acidity. In these cases, the concentrations of metals and chloride and water content in the organic phases were determined as described previously [19]: metals in the organic phases were stripped with acid or alkali and then metal concentrations in the aqueous solution were determined by titration with EDTA [14,20,21] except CyDTA for molybdenum [22], the chloride concentration by Volhard's method with nitrobenzene, and water content by Karl–Fischer titration [13].

Analysis

Thermogravimetry (TG) and differential thermal analysis (DTA) of the complexes were examined under an atmosphere of nitrogen. Heating rate and flow rate of nitrogen were 5°C min^{-1} and 50 cm^3 min^{-1}, respectively. The residues were derived from the complex by heating up to the required temperatures at a rate of 5°C min^{-1} under nitrogen atmosphere and then by

cooling immediately under the same atmosphere. Infrared spectra were recorded on a Japan Spectroscopic Co. Ltd. Model IRA-1 (4000–650 cm^{-1}) and IR-F (700–200 cm^{-1}) grating spectrometers. X-ray powder diffraction diagrams were obtained on a Geigerflex recording X-ray diffractometer with filtered copper radiation (generator operating at 30 kV and 15 mA, divergence slits $1 \times 1°$, receiving slit 0.3 mm, scanning speed 2° min^{-1}, chart speed 10 mm min^{-1}, time constant 2 s, scale factor 10, glancing angle 5°). The volatile matter generated during the DTA was collected in a 2 cm^3 syringe at the gas outlet of the DTA apparatus and analyzed with a Shimazu Model GC-6AMPTF gas chromatograph under the following analytical conditions: carrier gas, helium at 40 cm^3 min^{-1}; column, Porapak Q of 80/100 mesh; column temperature, 140°C; detector, FID. Each component detected was identified by gas chromatography–mass spectrometry (GC–MS). Hydrogen chloride in the volatile matter was trapped in a 10°C interval at temperatures between 200 and 350°C in 0.05 mol l^{-1} silver nitrate solution by means of passing through its solution for 3 min, and the concentration of chloride ion was determined by Volhard's method.

RESULTS AND DISCUSSION

Thermal decomposition of the complexes of divalent metals with TOA and TOMAC

The TG and DTA curves of divalent manganese, cobalt, copper and zinc complexes with TOA and TOMAC are shown in Figs. 1 and 2. The DTA curve of the manganese(II) complex with TOA exhibits three endotherms at 330, 370 and 630°C, respectively. In the TG curve, the weight loss of 87% is associated with the endotherms at 330 and 370°C, and a gradual weight loss is found above 630°C. By assuming that the complex $(R_3NH)_2MnCl_4$ is decomposed into manganese chloride ($MnCl_2$) at 300–400°C, its weight loss is calculated to be 86.1%, analogous to the observed value. Accordingly it might be explained that the endotherm at 630°C and the gradual weight loss above this temperature are ascribed to the melting of manganese chloride and the release of chlorine from the resulting chloride, respectively. According to Tello et al. [23], who have reported the thermal decomposition of manganese(II) complexes with primary amines, $(RNH_3)_2MnCl_4$, those complexes decompose in two steps:

$$(RNH_3)_2MnCl_4 \rightarrow RNH_3MnCl_3 + RNH_3Cl$$

$$RNH_3MnCl_3 \rightarrow RNH_3Cl + MnCl_2$$

In the TG curve of the complex $(R_3NH)_2MnCl_4$ (Fig. 1), however, such a decomposition process is not significantly confirmed.

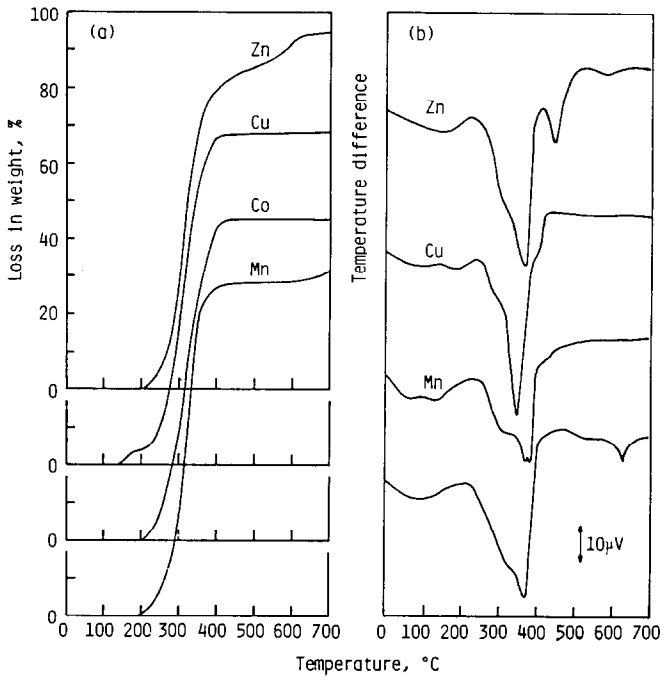

Fig. 1. TG (a) and DTA (b) curves of divalent metal complexes with TOA.

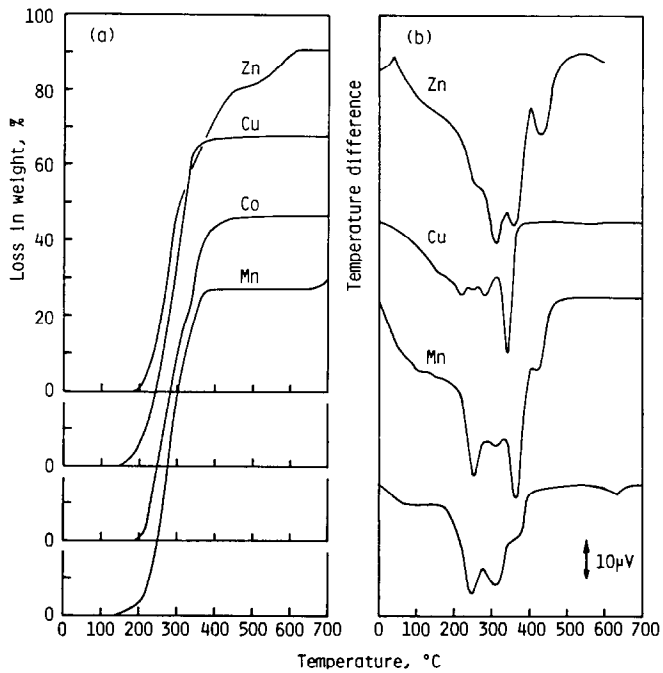

Fig. 2. TG (a) and DTA (b) curves of divalent metal complexes with TOMAC.

The DTA curve of the cobalt(II) complex with TOA shows endotherms at 300, 370, 385 and 420°C, which occur at near the point of changing shape of the TG curve (Fig. 1). From the TG curve it is deduced that the residues above 400°C exist as cobaltous chloride, $CoCl_2$. For the copper(II) complex with TOA, the DTA curve gives endotherms at 185, 300, 350 and 400°C, and the TG curve reveals a weight loss of 4% at 140–210°C, followed by one of 84% at 210–410°C. The weight loss at the first stage corresponds to the release of a molecule of chloride or hydrogen chloride. In the DTA curve of the zinc(II) complex with TOA the endotherms are observed at 320, 370, 450 and 580°C, and weight losses of 70, 13 and 9% are obtained at 230–400, 400–500 and 500–600°C, respectively, suggesting that the thermal decomposition of its complex proceeds in three stages.

The TG and DTA curves for divalent manganese, cobalt, copper and zinc complexes with TOMAC exhibit endotherms at 250, 315 and 370°C for manganese, 250, 315, 370 and 420 for cobalt, 215, 285, 325, 345 and 375°C for copper and 250, 310, 360 and 425°C for zinc. In the TG curves of the complexes of manganese, cobalt and zinc, a few inflection points appear in the temperature interval 200–400°C, suggesting that some reactions occur successively in this temperature range. The metal complexes with TOMAC begin to lose weight at a lower temperature than those with TOA: at 250°C the weight losses are 3.4–8.2 and 15.3–24.0% for the complexes with TOA and TOMAC, respectively. It is therefore presumed that the complexes with TOA are thermally more stable than those with TOMAC.

The volatile matter generated by the thermal decomposition of the metal complexes with TOA and TOMAC contains aliphatic compounds such as allene, ethylene, ethane, propene, propane, 1-butene, 2-butene and methyl chloride (identified by GC–MS), and hydrogen chloride (trapped in silver nitrate solution), for the complexes with TOA. The representative data of zinc complexes with TOA and TOMAC are given in Fig. 3, where the relative peak heights in the gas chromatogram for ethane and methyl chloride of the components and the relative amount of hydrogen chloride are plotted as a function of heating temperature. From this it is seen that the amounts of components detected above 250°C increase with increasing temperature in accordance with the weight loss in the TG curve, and that their maxima correspond with the endotherms in the DTA curve. The other detected hydrocarbons show a distribution analogous to ethane, and a similar trend is also observed for the other complexes. Further, it is found that hydrogen chloride evolved from the complexes with TOA is detected above 200°C (before detection of the organic components) and its maximum amount is obtained at about 250°C for all the complexes studied. It is therefore inferred that the thermal decomposition is initiated by the release of hydrogen chloride, and followed by the decomposition of TOA. This implies that in the DTA curves the endotherms at 330, 300, 300 and 370°C for divalent manganese, cobalt, copper and zinc complexes, respectively, are

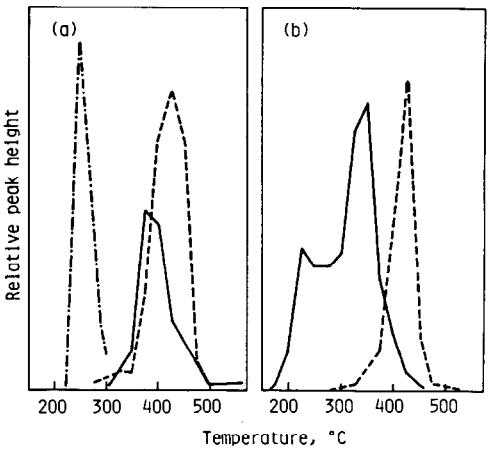

Fig. 3. Relative peak heights of C_2H_6 (— — —) and CH_3Cl (———) in the gas chromatograph and the relative amount of HCl (·–·–·) (determined by Volhard's method) as a function of heating temperature for zinc(II) chloro complexes with (a) TOA and (b) TOMAC.

assigned to the release of hydrogen chloride accompanied by the decomposition of TOA. Because the TG curve reveals weight losses > 5%, corresponding to the theoretical values for the thermal reaction of the complexes of divalent metals except copper

$$(R_3NH)_2MCl_4 \rightarrow (R_3N)_2 \cdots MCl_2 + 2HCl$$

and of the copper complex

$$(R_3NH)_2CuCl_4 \rightarrow (R_3N)_2 \cdots CuCl + 2HCl + (1/2)Cl_2$$

In addition it is considered that the endotherms at 370°C for manganese, 370 and 385°C for cobalt, 350°C for copper and 370 and 450°C for zinc arise from the cracking of alkyl groups.

The volatile matter for the complexes with TOMAC contains the same organic components as that of the complexes with TOA, although the former complexes have much more methyl chloride than the latter complexes. In Fig. 3, it is apparent that the distribution of methyl chloride is different from that of hydrocarbons. The maximum amount of methyl chloride is detected at 250, 250, 200 and 350°C for manganese, cobalt, copper and zinc, respectively. This component is mainly generated at the beginning of the thermal decomposition as shown in Fig. 3, implying that decomposition of the complexes with TOMAC is initiated by the evolution of methyl chloride.

Analytical data for the residues derived from the metal complexes with TOA by heating to the stated temperatures are indicated in Table 2. The molar ratio of the concentration of metal to that of chloride approaches 1 : 2 for manganese, cobalt and zinc and 1 : 0 for copper. It is thus postulated that all the metal complexes with TOA studied decompose into metal chloride,

TABLE 2

Composition of residues derived from divalent metal complexes with TOA on heating at the stated temperatures

Temp. (°C)	Molar ratio, [Cl]/[M]			
	Mn(II)	Co(II)	Cu(II)	Zn(II)
250	3.3	3.6	1.8	3.6
300	2.7	2.3	0.4	3.3
400	1.7	1.8	0	2.0
500	1.7	1.8	0	1.5

MCl_2, except that of copper which decomposes into metallic copper. These facts are also supported by the following results: in the X-ray diffraction diagrams for the cobalt(II) complex, the formation of cobaltous chloride hydrate is found on heating above 300°C (Table 3). For the copper(II) complex, the diffraction lines assigned to cupric chloride and metallic copper are observed at 300°C, and above 350°C those of metallic copper only remain. In contrast, no diffraction lines are recognized for the complexes of manganese(II) and zinc(II), although the residues produced by heating the former complex at the stated temperatures above 400°C for 2 h exhibit diffraction lines due to manganese chloride hydrate. In the infrared spectra of the residues for the manganese(II) complex, C–H stretching bands at 2920 and 2850 cm^{-1}, CH_3 degenerate and CH_2 scissoring bands at 1470 cm^{-1}, CH_3 symmetrical bending band at 1390 cm^{-1} and CH_2 rocking band at 730 cm^{-1} decrease in intensity at 300°C and disappear above 400°C, suggesting that the alkyl groups of TOA crack at temperatures between 300 and 400°C. The Mn–Cl stretching band at 284 cm^{-1} fades out at 400°C in accordance with decreasing bands due to alkyl groups. This indicates that the conformation of the original species is held below 400°C. On heating at 300°C, a strong band arising from the N–H stretching

TABLE 3

X-ray diffraction results for residues derived from divalent metal complexes with TOA by heating to the stated temperatures

Temp. (°C)	Phase detected			
	Mn(II)	Co(II)	Cu(II)	Zn(II)
300	– [a]	$CoCl_2 \cdot 6H_2O$	CuCl + Cu	Am
350	–	–	Cu	–
400	Am	$CoCl_2 \cdot 6H_2O$	Cu	Am
500	Am	$CoCl_2 \cdot 6H_2O$	Cu	Am

Am denotes amorphous.

[a] No detection.

TABLE 4

Probable assignment for endothermic reactions in the DTA curves of divalent metal complexes with TOA and TOMAC

Temperature (°C)								Probable assignment
Mn(II)		Co(II)		Cu(II)		Zn(II)		
TOA	TOMAC	TOA	TOMAC	TOA	TOMAC	TOA	TOMAC	
– [a]	–	–	–	185	218	–	–	Dechlorination
	250		250		250		260	Release of HCl and cracking
330		300		300		320		
					280			
	315		315				310	Cracking
370	360	370	370	350	345	370 [b]	355 [b]	
		385						
		420	420	400		450	425	
						580		
630	630							Melting

[a] No detection.

[b] This endotherm arises from cracking and melting of zinc chloride.

frequency at 2640 cm^{-1} disappears, and in addition C=C stretching and/or C=N stretching vibrations appear as a broad band centered around 1600 cm^{-1}. This means that a part of TOA is thermally decomposed and then an alkene and/or a C=N containing compound is formed. Above 400°C a broad band is observed at 600–450 cm^{-1}, assigned to the librational vibration of H_2O and Mn–Cl vibration of manganese chloride, $MnCl_2 \cdot xH_2O$ [24]. A similar trend is also observed for the cobalt(II) complex, but for the complexes of copper(II) and zinc(II) the bands due to alkyl groups disappear at 300 and 500°C, respectively. Thus it is considered that the thermal stability of these complexes is of the order of Cu < Mn ≃ Co < Zn. For the zinc(II) complex, the band at 275 cm^{-1} assigned to Zn–Cl stretching vibration of the original complex remains up to 300°C. Above 400°C the band due to Zn–Cl stretching vibration of zinc chloride, $ZnCl_2$ [23], appears at 500 cm^{-1}, accompanied by a two-step weight loss. This may be attributed to the fact that the melting point of zinc chloride formed by the thermal decomposition of the zinc complex with TOMAC is in the same temperature range as that in which the complex is thermally decomposed.

Hence the endothermic reactions in the DTA curves are assigned as given in Table 4, and accordingly it is considered that the thermal decomposition of the complexes of divalent metals with TOA proceeds in the following sequence:

$$(R_3NH)_2MCl_4 \xrightarrow{-HCl} [(R_3N)_2 \cdots MCl_2] \xrightarrow{\text{cracking}} MCl_2 + A' \xrightarrow{\text{cracking}} MCl_2$$

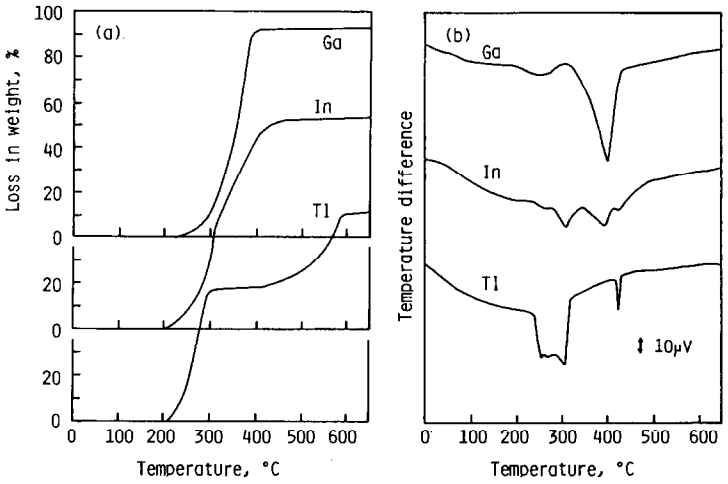

Fig. 4. TG (a) and DTA (b) curves of trivalent metal complexes with TOA.

except the copper complex, which is expressed as:

$$(R_3NH)_2CuCl_4 \xrightarrow{\text{reduction}} (R_3NH)_2CuCl_3 \xrightarrow{-HCl} [(R_3N)_2 \cdots CuCl]$$

$$\xrightarrow{\text{cracking}} CuCl + A' \xrightarrow{\text{reduction and cracking}} Cu$$

where A′ denotes the thermally decomposed product.

The endotherms in the DTA curve correspond to the distribution of methyl chloride and hydrocarbons (Figs. 3 and 4). Of the manganese(II) complex, the endotherms at 250, 315 and 370°C are assigned to dechlorination due to the evolution of methyl chloride, dechlorination and/or cracking, and cracking, respectively. The endothermic reactions in the DTA curves of other metal complexes are assigned as given in Table 5. From the results obtained by chemical analysis, X-ray diffraction and infrared spectroscopy, it is confirmed that the residues after decomposition above 300°C have the same composition as that described in the thermal decomposition of the manganese complex with TOA. For the complexes of manganese(II), cobalt(II) and zinc(II), metal chlorides such as $MnCl_2$, $CoCl_2$ and $ZnCl_2$ are produced, respectively, while for the copper(II) complex, metallic copper is formed via cuprous chloride.

Consequently the following process is deduced for the thermal decomposition of divalent metal complexes with TOMAC:

$$(R_3R'N)_2MCl_4 \xrightarrow{-CH_3Cl \text{ and cracking}} MCl_4 + A' \xrightarrow{\text{cracking}} MCl_2$$

TABLE 5

Relative peak heights of some components in the gas chromatogram of the chloro complex of gallium(III) with TOA as a function of heating temperature

Temp. (°C)	Relative peak height [a] (mm)						
	C_3H_4	C_4H_4	C_2H_6	C_3H_6	CH_3Cl	1-C_4H_8 [b]	2-C_4H_8 [b]
200	4						
225							
250	10		2		1		
275	8		2				
300	8		3		4		
325	15	10	4	3	8	11	23
350	14	6	9	9	17	6	5
375	12	12	4	60	64	42	20
400	102	352	210	1540	62	950	540
425	26	46	54	142	12	73	50
450	15	33	30	54	5	21	5
475	20	71	45	62	6	25	4
500	24	100	54	75		33	5

[a] Sensitivity range 4×10^3 μV.

[b] 1- or 2-C_4H_8 denotes 1- or 2-butene.

except that of the copper complex which is expressed as

$$(R_3R'N)_2CuCl_4 \xrightarrow{\text{reduction}} (R_3R'N)_2CuCl_3 \xrightarrow{-CH_3Cl \text{ and cracking}} CuCl + A'$$

$$\xrightarrow{\text{reduction and cracking}} Cu$$

Consequently the following structures, (**I**) and (**II**), are proposed for the chloro complexes of divalent metals formed in the extraction from hydrochloric acid solutions by TOA and TOMAC in benzene:

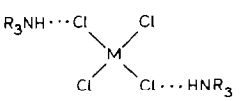

(I)

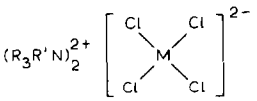

(II)

From the examination by spectrophotometry and electron spin resonance spectroscopy [25], it is observed that the M–Cl bond in the species $(R_3R'N)_2MCl_4$ is rather more ionic than that in the species $(R_3NH)_2MCl_4$, and the moiety MCl_4^{2-} with TOA is more flattened than that for TOMAC. These facts arise from the differences in their structures, (**I**) and (**II**), which are of tetrahedral geometry, formed during extraction according to solvating and anion-exchange reactions by TOA and TOMAC [26,27].

Thermal decomposition of the complexes of trivalent metals with TOA and TOMAC

The TG and DTA curves of trivalent gallium, indium and thallium complexes with TOA and TOMAC are shown in Figs. 4 and 5. For the complexes with TOA, the TG curves exhibit weight losses of 92.7% at 410°C for gallium, 89.0% at 440°C for indium, and 58.4% at 300–440°C and 92.2% at 585°C for thallium, while the DTA curves of the complexes reveal endothermic reactions at 270 and 400°C for gallium, 270, 310, 400 and 440°C for indium and 255, 270, 310 and 425°C for thallium. The complexes with TOMAC exhibit weight losses of 93.2% at 400°C for gallium, 92.0% at 470°C for indium, and 54.3% at 300–430°C and 86.4% at 580°C for thallium in the TG curves, and endotherms at 270, 400 and 410°C for gallium, 290, 350 and 440°C for indium and 255, 265, 300 and 425°C for thallium in the DTA curves. In Figs. 4 and 5 it is observed that the endothermic reactions in DTA occur near the point of changing shape in the TG curve. Additionally it is presumed that the thermal stability of the complexes with TOA resembles that of the complexes with TOMAC.

The volatile matter generated by the thermal decomposition of trivalent gallium, indium and thallium complexes with TOA and TOMAC is similar to that in the cases of divalent metal complexes: aliphatic compounds such as allene, ethylene, ethane, 1-butene, 2-butene and methyl chloride and hydrogen chloride. Some representative gas chromatographic data are illustrated for the gallium complexes with TOA and TOMAC in Tables 5 and 6, where the relative peak heights in the gas chromatogram for some of the components are indicated as a function of heating temperature. In addition, the variation of the molar ratios, [Cl]/[M] (M = Ga, In, Tl), in the residues derived from the complexes with TOA and TOMAC by heating to the stated temperatures is given in Table 7. Their molar ratios attain 3 : 1 for gallium

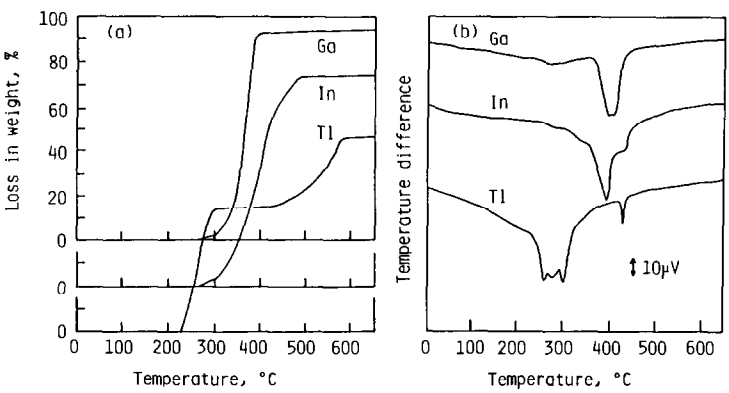

Fig. 5. TG (a) and DTA (b) curves of trivalent metal complexes with TOMAC.

TABLE 6

Relative peak heights of some components in the gas chromatogram of the chloro complexes of gallium(II) with TOMAC as a function of heating temperature

Temp. (°C)	Relative peak height [a] (mm)						
	C_3H_4	C_2H_4	C_2H_6	C_3H_6	CH_3Cl	1-C_4H_8 [b]	2-C_4H_8 [b]
200							
225		3			1		
250		3		5	2		
275	8	1	1		4		
300	16	3	3	6	32		
325	15	6	5	3	114		
350	10	5	4	2	95		
375	9	9	5	13	124	6	6
400	11	20	9	134	79	97	36
425	152	400	400	1100	280	512	290
450	28	56	46	136	82	27	57
475	5	9	7	21	9	8	1
500	4	3	3	8	7		

[a] Sensitivity range 4×10^3 μV.

[b] 1- or 2-C_4H_8 denotes 1- or 2-butene.

and indium, and 1 : 1 for thallium at 350°C. It is thus postulated that all the metal complexes with TOA and TOMAC studied decompose into metal chloride, MCl_3, except the thallium complexes which decompose to MCl. These facts are supported by the X-ray diffraction results (Table 8), in accordance with the infrared spectral ones. The X-ray results indicate that the residues produced by heating the complexes of gallium and indium with TOA and TOMAC are amorphous types independent of heating temperature, while those of thallium exhibit a pattern due to the reduction to

TABLE 7

Variation of molar ratios, [Cl]/[M] [a], in the residues derived from trivalent metal complexes with TOA and TOMAC by heating to the stated temperature

Temp. (°C)	Molar ratio [Cl]/[M]					
	Ga(III)		In(III)		Tl(III)	
	TOA	TOMAC	TOA	TOMAC	TOA	TOMAC
100	4.4	4.1	4.7	3.9	4.1	4.3
200	–	–	4.6	3.8	4.1	4.2
250	3.7	3.9	3.9	3.8	2.2	2.8
300	–	–	3.3	3.5	1.4	1.2
350	3.2	2.9	3.1	3.2	1.1	1.2
400	–	–	2.8	2.9	1.1	1.0

[a] M = Ga, In or Tl.

TABLE 8

X-ray diffraction results for the residues derived from trivalent metal complexes with TOA and TOMAC by heating to the stated temperature

Temp. (°C)	Phase detected					
	Ga(III)		In(III)		Tl(III)	
	TOA	TOMAC	TOA	TOMAC	TOA	TOMAC
200	–	–	Am	Am	TlCl	TlCl
250	Am	Am	Am	Am	TlCl	TlCl
300	–	–	Am	Am	TlCl	TlCl
350	Am	Am	Am	Am	TlCl	TlCl
400	–	–	Am	Am	Am	Am
450	–	–	Am	Am	Am	Am

Am denotes amorphous.

thallium(I) chloride at 200°C, although its pattern disappears on heating at 400°C. From these results it is seen that the amount of components detected above 250°C increases with increasing temperature, in accordance with the weight loss in the TG curve, and the maximum amount of their volatile matter corresponds to the endotherms in the DTA curve. In the DTA curves, the endotherms at 270, 270 and 255–270°C for trivalent gallium, indium and thallium complexes, respectively, are assigned to the release of hydrogen chloride accompanied by the decomposition of TOA. The TG curves reveal weight losses corresponding to theoretical values for the thermal reactions of complexes of trivalent metals with TOA.

$$(R_3NH)_nMCl_{3+n} \rightarrow [nR_3N \cdots MCl_3] + nHCl$$

where $n = 1$ and 2 for gallium and indium, except the thallium complex which may be expressed as

$$R_3NHTlCl_4 \rightarrow [R_3N \cdots TlCl] + HCl + 3/2Cl_2$$

The volatile matter for complexes with TOMAC contains the same organic components as that for the complexes with TOA, although the former complexes contain more methyl chloride than the latter complexes. As the release of methyl chloride occurs at the beginning of thermal decomposition, it is deduced that the endotherms at lower temperatures which appear in DTA for the complexes correspond to the distribution of methyl chloride and hydrocarbons. The endotherms at 270 and 380°C for gallium, 290 and 350°C for indium and 255 and 265°C for thallium are assigned to dechlorination due to the evolution of methyl chloride and/or cracking.

Accordingly it is concluded that the thermal decompositions of the complexes of trivalent metals with TOA and TOMAC proceed in the

following sequences: for the complexes with TOA

$$R_3NHGaCl_4 \xrightarrow[-HCl]{270°C} GaCl_3 + A' \xrightarrow[\text{cracking}]{300-400°C} GaCl_3$$

(thermal dissociation at ~ 400°C)

$$(R_3NH)_2InCl_5 \xrightarrow[-HCl]{270°C} InCl_3 + A' \xrightarrow[\text{cracking}]{300-400°C} InCl_3 \text{ (sublimation at } > 440°C)$$

and

$$R_3NHTlCl_4 \xrightarrow[\text{reduction and } -HCl]{255-270°C} TlCl + A' \xrightarrow[\text{cracking}]{\sim 300°C} TlCl \text{ (sublimation at 425°C)}$$

where A′ denotes the thermally decomposed product; for the complexes with TOMAC

$$R_3R'NGaCl_4 \xrightarrow[-CH_3Cl \text{ and cracking}]{270°C} GaCl_3 + A' \xrightarrow[\text{cracking}]{300-400°C} GaCl_3$$

(thermal dissociation at ~ 400°C)

$$R_3R'NInCl_4 \xrightarrow[-CH_3Cl \text{ and cracking}]{290-350°C} InCl_3 + A' \xrightarrow[\text{cracking}]{300-400°C} InCl_3$$

(sublimation at > 440°C)

and

$$R_3R'TlCl_4 \xrightarrow[\substack{-CH_3Cl \text{ and cracking} \\ \text{and/or reduction}}]{255-265°C} TlCl + A' \xrightarrow[\text{cracking}]{\sim 300°C} TlCl \text{ (sublimation at 425°C)}$$

supporting the proposed structures, (**III**) and (**IV**), which are in a tetrahedral arrangement, for the complexes with TOA and TOMAC:

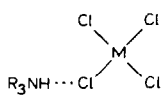

(III)

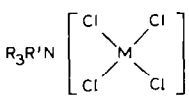

(IV)

in which M = Ga, In and Tl, except for the structure for the indium complex with TOA which has a tetrahedral bipyramidal or square pyramidal arrangement.

Thermal decomposition of the complexes of tetravalent metals with TOA and TOMAC

The TG and DTA curves of vanadyl complexes with TOA and TOMAC are shown in Fig. 6. In the complex with TOA, the TG curve exhibits weight losses of 81.6% at 300°C and 3.0% at 300–450°C, and the DTA curve gives endothermic reactions at 160, 220, 230, 285 and 305°C. The complex with TOMAC reveals weight losses of 81.4 and 5.2% at 300 and 300–450°C,

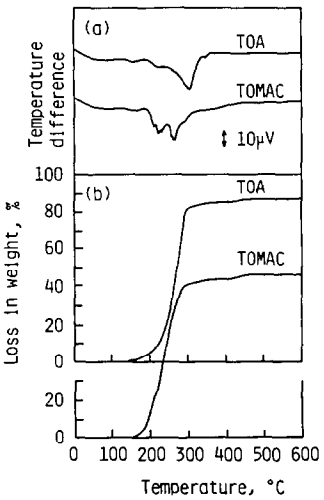

Fig. 6. DTA curves (a) and TG (b) curves of the vanadyl complexes with TOA and TOMAC.

respectively, in the TG curve and endotherms at 150, 210, 220, 235, 240, 255 and 270°C in the DTA curve. Additionally, from Fig. 6 it is observed that the endothermic reactions in the DTA curves occur near the point of changing shape in the TG curve.

The volatile matter generated by the thermal decomposition of the vanadyl complexes with TOA and TOMAC contains aliphatic compounds such as allene, ethylene, ethane, propene, propane, 1-butene, 2-butene, methyl alcohol and methyl chloride and hydrogen chloride. Some representative gas chromatographic data are illustrated in Tables 9 and 10, where the relative peak heights in the gas chromatogram for some components are indicated as a function of heating temperature. In addition, the change in molar ratios, [Cl]/[V], in the residues obtained by heating the complexes with TOA and TOMAC is given in Table 11. From these it is seen that the amount of components detected above 250°C increases with increasing temperature, in accordance with the weight loss in the TG curve, and the maximum amount of their volatile matter corresponds to the endotherms in the DTA curve. As indicated in the thermal decomposition of divalent metal complexes, hydrogen chloride evolved from the complex with TOA is detected above 200°C (before detection of the organic components) and its maximum amount is obtained at about 250°C. It is, therefore, inferred that the thermal decomposition is initiated by the release of hydrogen chloride, followed by the decomposition of TOA. This implies that in the DTA curve the endotherms at 220 and 230°C are assigned to the release of hydrogen chloride accompanied by the decomposition of TOA. TG reveals a weight loss corresponding to the theoretical value for the thermal reaction of the complex with TOA.

$$R_3NHVO(OH)Cl_2 \rightarrow [R_3N \cdots VO(OH)Cl] + HCl$$

TABLE 9

Relative peak heights of some components in the gas chromatograph of the vanadyl complex with TOA as a function of heating temperature

Temp. (°C)	Relative peak height [a] (mm)					
	C_3H_4	C_2H_4	C_2H_6	C_3H_6	CH_3OH	CH_3Cl
150	7					
175	5				1	
200	7	1	1	2		
225				1		
250	14	2	3	2	3	1
275	13	2	3	2	2	1
300	10	3	4	3	2	1
325	37	6	10	3	9	5
350	33	12	11	2	12	3
375	28	14	12	2	12	
400	29	23	27	2		22
425	23	15	19	2		14
450	48	49	43	3		22
475	22	23	15	1		
500	27	22	13	2		

[a] Sensitive range 4×10^3 μV.

TABLE 10

Relative peak heights of some components in the gas chromatograph of vanadyl complexes with TOMAC as a function of heating temperature

Temp. (°C)	Relative peak height [a] (mm)					
	C_3H_4	C_2H_4	C_2H_6	C_3H_6	CH_3OH	CH_3Cl
150	5				17	
175	7	1		2	336	
200	16	3		3	2500	
225	12	2	1	3	270	
250	7	3	3	3	18	1550
275	10	2	6		10	3700
300	15	6	10			420
325	33	8	12	3	12	104
350	42	14	23	3	24	50
375	62	38	54	3	47	26
400	73	61	91	3	64	12
425	53	40	77	5	53	6
450	102	57	141	2	70	9
475	26	9	12	3	7	1
500		32	36	1	8	

[a] Sensitive range 4×10^3 μV.

TABLE 11

Composition of the residues from the vanadyl complexes with TOA and TOMAC by heating to the stated temperatures

Temp. (°C)	Molar ratio, [Cl]/[V]	
	TOA	TOMAC
150	2.0	1.9
200	1.8	1.7
250	1.1	1.1
300	0.7	0.3
350	0.2	0.1
400	0	0
500	0	0

where the conformation of the original species, VO(OH)Cl, may be formed during the thermal decomposition of the amine [5]. In addition, it is considered that the endotherm at 305°C arises from the cracking of the alkyl group.

The volatile matter for the complex with TOMAC contains the same organic components as that for the complex with TOA, although the former complex contains much more methyl alcohol and methyl chloride than the latter complex. In contrast, the thermal decomposition of divalent metal complexes with TOA and TOMAC does not indicate the release of methyl alcohol, attributed to the absence of hydrolyzed species [12]. In Table 10, it

TABLE 12

Probable assignment of the endothermic reactions in the DTA curves of the vanadyl complexes with TOA and TOMAC

Temp. (°C)		Probable assignment
TOA	TOMAC	
	150	Dissociation and/or dehydration
160		
	210 220 235 240	Release of CH_3OH
220 230		Release of HCl
	255 270	Release of CH_3Cl and cracking
285 305		Release of HCl and cracking

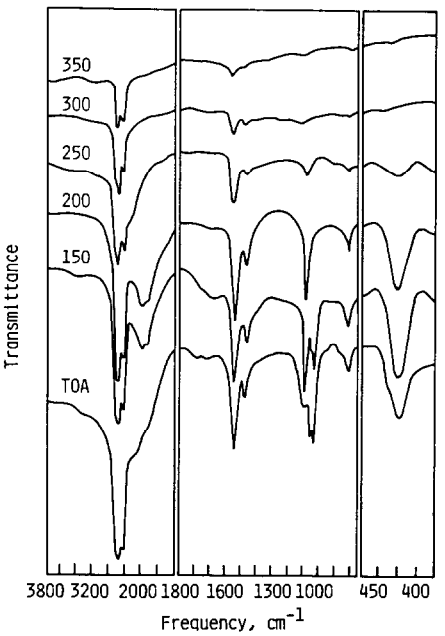

Fig. 7. Infrared spectra of the residues from the vanadyl complex with TOA by heating to the stated temperatures (numbers on curves are heating temperatures, °C).

is apparent that the distribution of methyl alcohol and methyl chloride is different from that of hydrocarbons: the maximum amounts of methyl alcohol and methyl chloride are detected at 200 and 275°C, respectively, and those of hydrocarbons at 400–450°C. These components are largely generated at the beginning of thermal decomposition, implying that the decomposition of the complex with TOMAC releases methyl alcohol at first and then methyl chloride. From this it is deduced that the endotherms in DTA correspond to the distribution of methyl alcohol, methyl chloride and hydrocarbons. The endotherms at 210, 220, 235 and 240°C are assigned to the release of methyl alcohol, and those at 255 and 270°C to dechlorination due to the evolution of methyl chloride and/or cracking (Table 12).

In the infrared spectrum of the vanadyl complex with TOA (Fig. 7), the absorptions assigned to the stretching frequency of the vanadyl group [21,28] appear at 1005, 970, 954 and 935 cm^{-1} as a quartet band, indicating a lowering in symmetry; the NH^+ stretching vibration at 2350 cm^{-1} in TOA hydrochloride shifts to a broad band centered around 3000 cm^{-1} and the V–Cl stretching vibration appears at 430 cm^{-1}, confirming formation of the chloro complex; absorption of the OH stretching band appears at 3400 cm^{-1} and the OH bending bands occur at 1735 and 1620 cm^{-1}, implying the presence of the hydrolyzed species. When the complex is heated at 150°C, the V–O stretching vibration appears at 1000 cm^{-1}, and simulta-

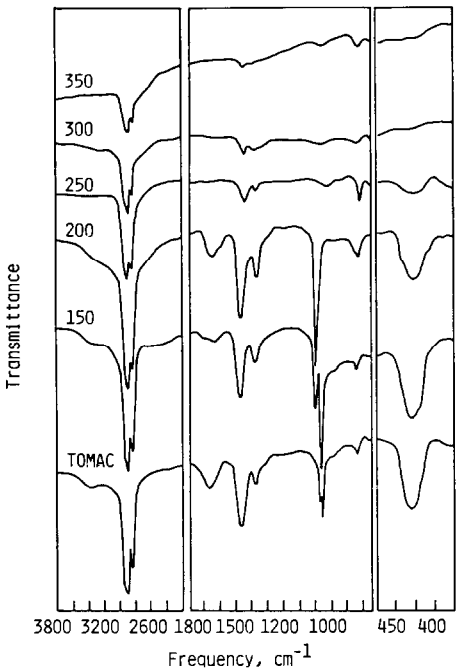

Fig. 8. Infrared spectra of the residues from the vanadyl complex with TOMAC by heating to the stated temperatures (numbers on curves are heating temperatures, °C).

neously the vanadyl group absorptions at 1005, 970, 954 and 935 cm^{-1} decrease in intensity; in addition, the NH^+ stretching band at 3000 cm^{-1} shifts to lower frequency at 2640 cm^{-1}. This is thought to result from dissociation of the dimeric complex, corresponding to the TG curve which exhibits a weight loss. The vanadyl group absorptions and the OH bands almost disappear at 200°C. On heating at 250°C, the NH^+ band, the C–H stretching bands at 2920 and 2860 cm^{-1}, the CH_3 degenerate (and CH_2 scissoring) and symmetrical bending modes at 1465 and 1380 cm^{-1} and the V–Cl stretching band decrease in intensity. In contrast, the vanadyl complex with TOMAC (Fig. 8) gives an infrared spectrum similar to that of the complex with TOA, except for the absence of the NH^+ stretching band. However, since the splitting in the V=O stretching bands at 968 and 955 cm^{-1} is less than that for the TOA complex, it is inferred that the symmetry of the latter is lower than that of the former. Changes in the infrared spectra of the thermally decomposed residues derived from the TOMAC complex are almost the same as those from the TOA complex.

Hence the endothermic reactions in the DTA curves are interpreted as given in Table 12. Furthermore the X-ray diffraction results indicate that the residues produced by heating the vanadyl complexes with TOA and TOMAC are amorphous types independent of heating temperature. In the thermal

decomposition of their complexes in air, however, the X-ray results reveal the pattern of V_2O_3 at 300°C and of V_2O_5 on further heating [5]. It is thus presumed that V_2O_3 is also formed during the decomposition process of their complexes under an atmosphere of nitrogen. Accordingly it is concluded that the thermal decomposition of the vanadyl complexes with TOA and TOMAC proceeds in the sequence

$$(R_3NHVO(OH)Cl_2)_2 \xrightarrow[\text{dissociation}]{\sim 160^\circ C} R_3NHVO(OH)Cl_2 \xrightarrow[-\text{HCl and cracking}]{200-300^\circ C} V_2O_3$$

and

$$(R_3R'NVO(OH)Cl_2)_2 \xrightarrow[\text{dissociation}]{\sim 150^\circ C} R_3R'NVO(OH)Cl_2 \xrightarrow[-CH_3OH, -CH_3Cl \text{ and cracking}]{200-300^\circ C} V_2O_3$$

supporting the proposed structures, (**V**) and (**VI**), for the vanadyl complexes with TOA and TOMAC.

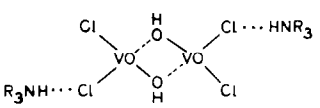

(V)

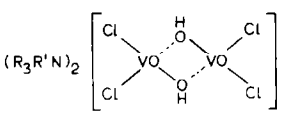

(VI)

On the other hand the complex with TOA or TOMAC gave the components zirconium : chloride : TOA or TOMAC in the molar ratio 1 : 6 : 2 (exactly 1 : 5.86 : 2.15 for TOA and 1 : 6.10 : 2.02 for TOMAC), indicating the composition $(R_3NH)_2ZrCl_6$ or $(R_3R'N)_2ZrCl_6$. The infrared spectra of the complexes showed no absorption caused by the OH groups, indicating that the complexes contain no coordinated water, and this was confirmed by Karl–Fischer titration. In addition, the infrared spectra of the zirconium complexes with TOA and TOMAC exhibit absorption bands at 295 and 300–280 cm^{-1}, respectively, assigned to the Zr–Cl stretching frequency, corresponding to the result [29] that the ν_3 frequency for the anionic hexahalides, $ZrCl_6^{2-}$, appears at 297–276 cm^{-1}, but for the compound $ZrCl_4$ at 423–421 cm^{-1}.

Hence the structures (**VII**) and (**VIII**), displaying a coordination number of six for zirconium (a point group O_h symmetry) are proposed for the complexes.

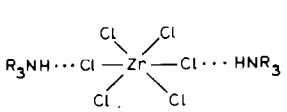

(VII)

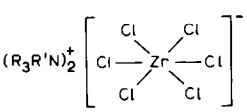

(VIII)

Thermal decomposition of the complexes of hexavalent metals with TOA and TOMAC

In the complex with TOA (Fig. 9), the TG curve exhibits weight losses of 73.4% at 200–300°C and 3.6% at 300–470°C, and the DTA curve gives endothermic reactions at 270, 305 and 330°C. The complex with TOMAC (Fig. 9) reveals a weight loss of 74.3% at 200–350°C in the TG curve and endotherms at 250, 265, 280 and 305°C, in the DTA curve. Additionally, it is observed that the endothermic reactions in the DTA curve occur near the point of changing shape of the TG curves.

The volatile matter generated by the thermal decomposition of the uranyl complexes with TOA and TOMAC contains aliphatic compounds such as allene, ethylene, ethane, propene, propane, 1-butene, 2-butene, methyl chloride (Tables 13 and 14) and hydrochloric acid. In addition, the change in molar ratios, [Cl]/[U], examined for the residues obtained by heating the complexes with TOA and TOMAC indicated that the amount of components detected above 250°C increases with increasing temperature, in accor-

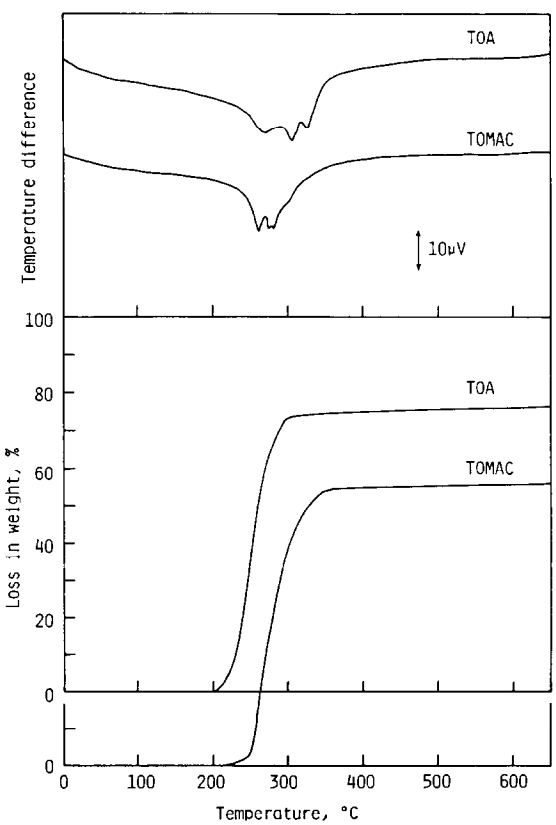

Fig. 9. TG and DTA curves of the chloro complexes of uranium(VI) with TOA and TOMAC.

TABLE 13

Relative peak heights of some compounds in the gas chromatogram of the chloro complex of uranium(VI) with TOA as a function of heating temperature

Temp. (°C)	Relative peak height [a] (mm)						
	C_3H_4	C_2H_4	C_2H_6	C_3H_6	CH_3Cl	1-C_4H_8 [b]	2-C_4H_8
200							
225							
250	70	2	2				
275		7	8	4	3	1	2
300	28	6	7	2	4	2	2
325	26	5	7	2	5	3	3
350	17	16	14	2	12	10	6
375	26	32	19	1	22	16	8
400	16	21	22		16	18	9
425	30	23	39	1	35	14	15
450	55	25	50		22	9	7
475	105	44	57			10	5
500	59	34	20		6	7	

[a] Sensitive range 4×10^3 μV.

[b] 1- or 2-C_4H_8 denotes 1- or 2-butene.

dance with the weight loss in TG, and the maximal amount of their volatile matter corresponds with the endotherms in DTA (Table 15). It is thus considered that in the DTA curve the endotherm at 270°C is assigned to the

TABLE 14

Relative peak heights of some compounds in the gas chromatogram of the chloro complex of uranium(VI) with TOMAC as a function of heating temperature

Temp. (°C)	Relative peak height [a] (mm)						
	C_3H_4	C_2H_4	C_2H_6	C_3H_6	CH_3Cl	1-C_4H_8 [b]	2-C_4H_8
200							
225					264		
250	12	4	3	3	1070	3	2
275	192	11	14	6	5200	10	9
300	35	8	8	5	194	3	4
325	17	5	6	2	55	3	5
350	17	7	7	1	13	9	8
375	19	12	12	2	34	11	9
400	45	53	50	1	22	33	19
425	30	36	34	1		18	15
450	28	37	35			15	10
475	22	55	24			35	7
500	18	30	15			20	3

[a] Sensitive range 4×10^3 μV.

[b] 1- or 2-C_4H_8 denotes 1- or 2-butene.

TABLE 15

Variation of molar ratios, [Cl]/[U], in the residues derived from the chloro complexes of uranium with TOA and TOMAC by heating to the stated temperature

Temp. (°C)	Molar ratio, [Cl]/[U]	
	TOA	TOMAC
100	4.0	3.9
200	3.6	3.6
250	2.9	2.2
300	2.2	0.8
350	0.8	0.2
400	0	0

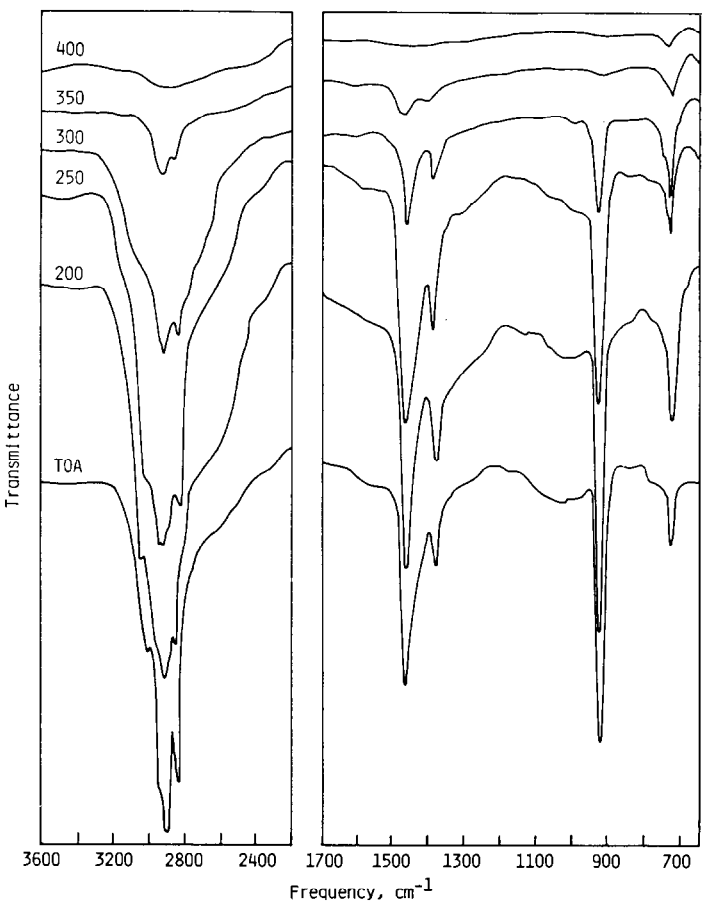

Fig. 10. Infrared spectra of the residues from the chloro complexes with TOA by heating to the stated temperatures (numbers on curves are heating temperatures, °C).

release of hydrochloric acid accompanied by the decomposition of TOA, and that the endotherms at 305 and 330°C arise from cracking of the alkyl group and dechlorination, respectively.

The volatile matter for the complex with TOMAC contains the same organic compounds as that for the complex with TOA, although the former complex contains much more methyl chloride than the latter complex. Moreover it is found that the distribution of methyl chloride is different from that of hydrocarbons: the maximal amount of methyl chloride is detected at 250–275°C, and that of hydrocarbons at 275–400°C. These components are mostly generated at the beginning of thermal decomposition, implying that the decomposition of the complex with TOMAC at first releases methyl chloride. From this the endotherms at 250 and 265°C are assigned to the release of methyl chloride, and those at 280 and 305°C to cracking and dechlorination, respectively.

In the infrared spectrum of the uranyl complex with TOA (Fig. 10), the absorption at 910 cm^{-1} is assigned to the asymmetric stretching frequency of the UO_2^{2+} group [30]; the NH^+ stretching vibration at 2350 cm^{-1} in TOA · HCl shifts to a broad band centered around 3000 cm^{-1}. On heating at 250°C, the NH^+ band, the C–H stretching bands at 2920 and 2860 cm^{-1}, the CH_3 degenerate (and CH_2 scissoring) and symmetrical bending modes at 1465 and 1380 cm^{-1} decrease in intensity, and at 400°C disappear. The uranyl complex with TOMAC gives an infrared spectrum similar to that of the complex with TOA, except for the absence of the NH^+ stretching band.

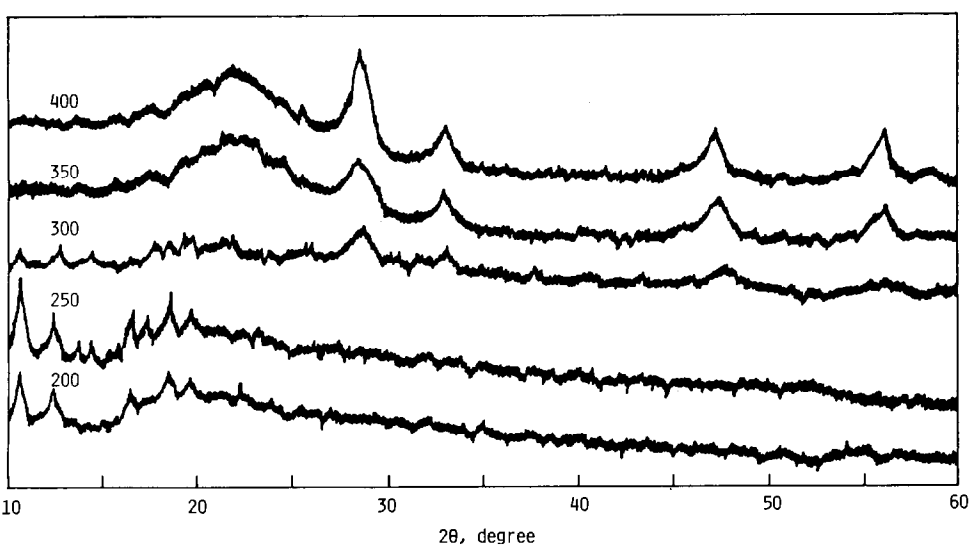

Fig. 11. X-ray diffraction diagrams of the residues derived from the chloro complex of uranium(VI) with TOA by heating to the stated temperatures (numbers on curves are heating temperatures, °C).

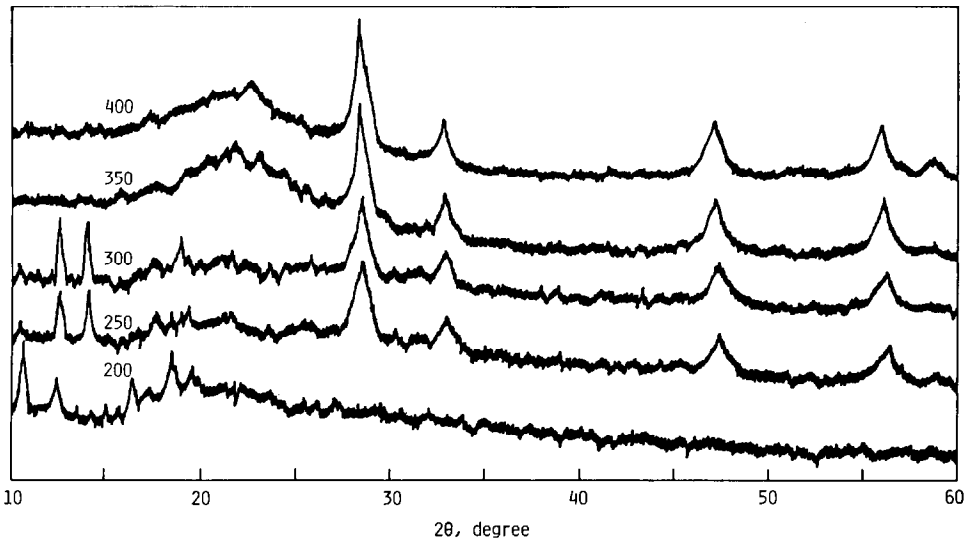

Fig. 12. X-ray diffraction diagrams of the residues derived from the chloro complex of uranium(VI) with TOMAC by heating to the stated temperatures (numbers on curves are heating temperatures, °C).

In addition the changes in the infrared spectra of the thermally decomposed residues derived from the TOMAC complex are almost the same as those from the TOA complex. Furthermore the X-ray diffraction results (Figs. 11 and 12, and Table 16) for the residues produced by heating the uranyl complexes with TOA and TOMAC indicated the following patterns: UO_2Cl_2, $UO_2Cl_2 + UO_2$ and UO_2 from the complex with TOA at 250, 300 and 350°C, respectively; UO_2Cl_2, $UO_2Cl_2 + UO_2$ and UO_2 from the complex with TOMAC at 200, 250 and 350°C, respectively. It is thus presumed that UO_2Cl_2 and UO_2 are formed during the decomposition process of their complexes under an atmosphere of N_2. Accordingly it is concluded that the

TABLE 16

X-ray diffraction results for the residues derived from the chloro complexes of uranium(VI) with TOA and TOMAC by heating to the stated temperature

Temp. (°C)	Phase detected	
	TOA	TOMAC
200	UO_2Cl_2	UO_2Cl_2
250	UO_2Cl_2	$UO_2Cl_2 + UO_2$
300	$UO_2Cl_2 + UO_2$	$UO_2Cl_2 + UO_2$
350	UO_2	UO_2
400	UO_2	UO_2
500	UO_2	UO_2

TABLE 17

Probable assignments of the endothermic reactions in the DTA curves of the chloro complexes of uranium(VI) with TOA and TOMAC

Temp. (°C)		Probable assignment
TOA	TOMAC	
	250 \ 265 /	Release of CH_3Cl
270		Release of HCl
305	280	Cracking
330	305	Dechlorination

thermal decompositions of the uranyl complexes with TOA and TOMAC proceed in the sequences

$$(R_3NH)_2UO_2Cl_4 \xrightarrow[-\text{HCl and cracking}]{250-320^\circ C} UO_2Cl_2 \xrightarrow[\text{dechlorination}]{320-360^\circ C} UO_2$$

and

$$(R_3R'N)_2UO_2Cl_4 \xrightarrow[-CH_3Cl \text{ and cracking}]{200-280^\circ C} UO_2Cl_2 \xrightarrow[\text{dechlorination}]{280-325^\circ C} UO_2$$

supporting the proposed structures, (**IX**) and (**X**), for the uranyl complexes with TOA and TOMAC.

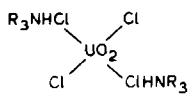

(IX)

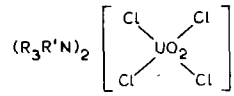

(X)

For the complexes of molybdenum(VI) with TOA and TOMAC at low aqueous acidity the TG curve of the complex with TOA reveals a weight loss of 53.5% at 175–750°C, and its DTA curve exhibits endotherms at 65, 100, 230, 265, 300 and 410°C. The complex with TOMAC gives a weight loss in the TG curve of 51.5% at 165–520°C and the DTA curve shows endotherms at 40, 80, 165, 270, 305 and 410°C. The volatile matter generated by the thermal decomposition of their complexes contains methyl alcohol detected at 350 and 275–300°C for TOA and TOMAC complexes, respectively, and hydrocarbons exhibiting maxima at 325–450°C and 400–475°C for TOA and TOMAC complexes, respectively. In contrast, the complexes with TOA and TOMAC prepared at higher aqueous acidity give the following thermoanalytical results: for the TOA complex, the TG curve reveals weight losses of 69.3 and 13.9% at 140–350 and 350–550°C, respectively, and the DTA curve shows endotherms at 80, 180, 275, 315 and 370°C; for the TOMAC complex, the TG curve shows weight losses of 60.2 and 15% at 85–350 and 350–650°C, respectively, and the DTA curve shows endotherms at 80, 115,

180, 270, 315 and 360°C. The volatile matter from the complex with TOA contains aliphatic compounds and hydrogen chloride. In contrast, although the volatile matter for the complex with TOMAC contains the same organic components as that for the complex with TOA, the former complex contains much more methyl chloride than the latter complex and does not release hydrogen chloride. In addition, the complexes with TOA and TOMAC formed at higher aqueous acidity do not release methyl alcohol because of the absence of hydrolyzed species.

The infrared spectra of the complexes at low aqueous acidity exhibit the following absorptions [21,31–34] in addition to absorptions of the alkyl groups due to TOA or TOMAC: for the complex with TOA, the broad band at 3020–2520 cm^{-1} due to the NH^+ stretching frequency, the Mo=O stretching band at 960–900 cm^{-1}, the Mo–OMo symmetric stretching and/or Mo–O stretching band at 840–670 cm^{-1}, the MoO_2 bending and deformation bands at 468–353 and 267–247 cm^{-1}, respectively, and Mo–OH stretching band at 605–522 cm^{-1}; for the complex with TOMAC, the Mo=O stretching band at 965–910 cm^{-1}, the Mo–O–Mo asymmetric stretching and/or Mo–O stretching bands at 835–661 cm^{-1}, the MoO_2 bending and deformation bands at 435–355 and 290–278 cm^{-1}, respectively, and additionally the Mo–OH stretching band at 597–520 cm^{-1}. The spectra of the complexes with TOA and TOMAC at higher aqueous acidity reveal the following absorptions: for the complex with TOA, the NH^+ stretching band centered around 2600 cm^{-1}, the Mo=O stretching bands at 965 and 920 cm^{-1}, the Mo–O–Mo and/or Mo–O stretching bands at 810, 730 and 705 cm^{-1} and the MoO_2 bending and deformation band at 420 (or 389) and 266 (or 249) cm^{-1}, respectively; for the complex with TOMAC, the Mo=O stretching bands at 950 and 910 cm^{-1}, the Mo–O–Mo and/or Mo–O stretching bands at 695 cm^{-1} and the MoO_2 bending and deformation bands at 389 and 265 (or 248) cm^{-1}, respectively. As their spectra do not exhibit the absorption due to the Mo–OH stretching frequency, it is expected that neither complex prepared at higher acidity possesses the OH group. On heating, those absorption patterns show changes in accordance with the results for thermal analysis.

Consequently the probable structures for their complexes are proposed on the basis of the results obtained [35].

CONCLUSION

When solvent-extracted metal complexes with TOA and TOMAC from hydrochloric acid solutions are thermally decomposed, it is found that the thermal decomposition behavior of the complexes with TOA is different from that with TOMAC. The complexes with TOA are initiated by the release of hydrogen chloride, and followed by the exhaust of hydrocarbons

due to the decomposition of TOA, while the complex with TOMAC exhausts methyl chloride in the beginning of the thermal decomposition and then hydrocarbons attributed to the decomposition of TOMAC. Further the complexes with TOMAC possessing a hydrolyzed group reveal the release of methyl alcohol accompanied by methyl chloride, as indicated in the thermal decomposition of the complexes of vanadium(IV) and molybdenum(VI). It is thus considered that the thermal decomposition behavior of these complexes is a result of the different structures, prepared in the extractions according to solvating and exchange reactions.

ACKNOWLEDGMENTS

The author wishes to thank Dr. H. Watanabe, Dr. T. Nakamura and Mr. Takahashi for assistance with part of the experimental work, and also the Research and Development Laboratory, Swiss Aluminium Ltd., Neuhausen, Switzerland, for the gift of gallium metal, and Koei Chemical Co., Ltd. for samples of TOA and TOMAC.

REFERENCES

1 T. Sato, J. Inorg. Nucl. Chem., 26 (1964) 2229; 27 (1965) 240.
2 T. Sato and T. Nakamura, Thermochim. Acta, 47 (1981) 189.
3 T. Sato and K. Adachi, J. Inorg. Nucl. Chem., 31 (1969) 1395.
4 T. Sato and H. Watanabe, Thermochim. Acta, 31 (1979) 159.
5 T. Sato, T. Nakamura and H. Watanabe, Anal. Chim. Acta, 98 (1978) 365.
6 T. Sato, T. Nakamura and T. Takahashi, J. Therm. Anal., 30 (1985) 97.
7 T. Sato, Anal. Chim. Acta, 77 (1975) 344.
8 T. Sato and T. Takahashi, Proc. 8th Int. Conf. on Thermal Analysis, Bratislava, 1985, Vol. 1, p. 668.
9 T. Sato, K. Adachi, T. Kato and T. Nakamura, Sep. Sci. Technol., 17 (1982) 1565.
10 T. Sato, T. Shimomura, S. Murakami, T. Maeda and T. Nakamura, Hydrometallurgy, 12 (1984) 245.
11 T. Sato, T. Nakamura and S. Ishikawa, Solvent Extr. Ion Exch., 2 (1984) 353.
12 T. Sato, S. Ikoma and T. Nakamura, J. Inorg. Nucl. Chem., 39 (1977) 395.
13 T. Sato and H. Watanabe, Anal. Chim. Acta, 49 (1970) 463.
14 T. Sato and H. Watanabe, Anal. Chim. Acta, 54 (1971) 439.
15 T. Sato, J. Inorg. Nucl. Chem., 28 (1966) 1461.
16 T. Sato, J. Appl. Chem., 16 (1966) 143.
17 T. Sato, J. Inorg. Nucl. Chem., 34 (1972) 3835.
18 T. Sato and H. Watanabe, Proc. Symp. Solvent Extr., 1984, Hamamatsu, p. 1.
19 E.g., T. Sato, J. Appl. Chem. Biotechnol., 22 (1972) 1233; T. Sato and M. Yamatake, Z. Anorg. Allg. Chem., 391 (1972) 174; T. Sato, M. Kuwahara, T. Nakamura and M. Ueda, J. Appl. Chem. Biotechnol., 29 (1979) 39.
20 (a) H. Flaschka, Chem. Anal., 42 (1953) 56; (b) J. Kinnunen and B. Wennerstrand, Chem. Anal., 46 (1956) 102.
21 T. Sato and T. Takeda, J. Inorg. Nucl. Chem., 32 (1970) 387.

22 R. Pribil and V. Vesely, Talanta, 17 (1970) 170.
23 M.J. Tello, E.H. Bocanegra and M.A. Arrandiaga, Thermochim. Acta, 11 (1975) 96.
24 J.R. Ferraro, Low-Frequency Vibrations of Inorganic and Coordination Compounds, Plenum Press, New York, 1971, p. 140.
25 T. Sato and T. Nakamura, J. Chem. Tech. Biotechnol., 34A (1984) 375.
26 T. Sato, T. Nakamura and T. Fujimatsu, Solvent Extr. Ion Exch., 1 (1983) 709.
27 T. Sato, T. Nakamura and M. Kuwahara, Solvent Extr. Ion Exch., 3 (1985) 283.
28 E.g., P.A. Kilz and D. Nicholls, J. Chem. Soc. A, (1966) 1175; J. Selbin, L.H. Holmes, Jr. and S.P. McGlynn, J. Inorg. Nucl. Chem., 25 (1963) 1359; D.N. Salhyanarayana and C.C. Patel, J. Inorg. Nucl. Chem., 30 (1968) 207.
29 Low-Frequency Vibrations of Inorganic and Coordination Compounds, Plenum Press, New York, 1971, pp. 121, 128.
30 E.g., B.M. Gatehouse and A.E. Comyns, J. Chem. Soc., (1958) 3965; G.L. Caldow, A.B. Van Cleave and R.L. Eager, Can. J. Chem., 38 (1960) 772.
31 F.W. Moore and R.E. Rice, Inorg. Chem., 7 (1968) 2510.
32 W.P. Griffith and T.D. Wickins, J. Chem. Soc. A, (1967) 675; (1968) 400.
33 D.A. Adams, R.G. Adams and R.G. Churchill, J. Chem. Soc. A, (1968) 2310.
34 Low-Frequency Vibrations of Inorganic and Coordination Compounds, Plenum Press, New York, 1971, p. 101.
35 T. Sato, H. Watanabe and T. Takahashi, Proc. Symp. of Studies on the Structure and Reaction of Metal Complex and its Thermal Energy, Hamamatsu, 1986, p. 106.